

ISSN: 0256-307X

中国物理快报

Chinese Physics Letters

Volume 29 Number 12 December 2012

A Series Journal of the Chinese Physical Society
Distributed by IOP Publishing

Online: <http://iopscience.iop.org/cpl>
<http://cpl.iphy.ac.cn>

CHINESE PHYSICAL SOCIETY
IOP Publishing

JUST FOR AUTHORS
— CHINESE PHYSICS LETTERS

Ultrastable Fiber-Based Time-Domain Balanced Homodyne Detector for Quantum Communication *

WANG Xu-Yang(王旭阳), BAI Zeng-Liang(白增亮), DU Peng-Yan(杜鹏燕),
LI Yong-Min(李永民)**, PENG Kun-Chi(彭堃焯)

State Key Laboratory of Quantum Optics and Quantum Optics Devices, Institute of Opto-Electronics,
Shanxi University, Taiyuan 030006

(Received 25 June 2012)

We present an ultrastable fiber-based time-domain balanced homodyne detector which can be used for precise characterization of pulsed quantum light fields. A variable optical attenuator based on bending the fiber is utilized to compensate for the different quantum efficiencies of the photodiodes precisely, and a common mode rejection ratio of above 76 dB is achieved. The detector has a gain of $3.2 \mu\text{V}$ per photon and a signal-to-noise ratio above 20 dB. Optical pulses with repetition rates up to 2 MHz can be measured with a detection efficiency of 66%. The stability of the detector is analyzed via an Allan variance measurement and the detector exhibits superior stability which enables a 100-s window for measurement without calibration.

PACS: 42.50.Dv, 03.67.Hk

DOI: 10.1088/0256-307X/29/12/124202

Time-domain shot noise limited balanced homodyne detectors (BHD) can give the field quadrature values of pulsed quantum light fields directly and play an important role in quantum communication^[1–4] and quantum tomography,^[5–8] etc. With the rapid progress in quantum information science, the time-domain BHDs have attracted more attention. For example, in all-fiber continuous variable quantum key distribution systems, where the receiver Bob needs to measure the quadratures of the signal field in which random numbers are encoded, fiber-based BHDs with high stability, low electronic dark noise, high common mode rejection ratio (CMRR) are required.

The time-domain BHDs can be divided into two types according to the different ways of integrating the difference photon-current produced by the two photodiodes, one is based on charge sensitive preamplifier (CSP),^[5,9–11] and the other is based on a transimpedance preamplifier (TP) or voltage preamplifier (VP).^[12–16] For the CSP BHDs, the photon-current is integrated on the feedback capacitor of the CSP and the peak value of the BHD output pulse is linearly proportional to the quadrature value of the signal field. The first time-domain shot noise limited BHD was based on CSP, it has a subkilohertz repetition rate and a shot noise to electronic noise ratio of 9 dB.^[5] Hansen *et al.*^[9] also built a BHD of this type working at a repetition rate of 204 kHz with a shot noise to electronic noise ratio of 14 dB.

For TP or VP BHDs, when the pulse duration of the incident light is much longer than the response time of the photodiode,^[12] and the field quadrature

value is proportional to the area under each output electric pulse, one has to collect plenty of data points for each pulse and sum the sample points together to acquire a single value of the signal field quadrature. Although this kind of BHD allows a repetition rate above tens of MHz, high speed data acquisition which should be much higher than the pulse repetition rate and post-processing are necessary. This is quite different from that of a CSP BHD where only the peak value of the output electric pulse is measured and the system cost and complexity can be decreased significantly. For TP or VP BHDs, there also exists another kind of situation where the pulse duration of the input light is shorter than the response time of the photodiode.^[13–16] In such a situation, the photodiode's junction capacitance will integrate the difference photon-current and the peak value of output electric pulse is proportional to the signal field's quadrature value. It is known that good linearity is necessary to ensure that the BHD output is proportional to the signal field quadrature. However, when very short optical pulses are incident on the photodiodes, the high peak power will saturate the photodiodes easily and also lead to poor matching of the photodiode responses.^[12]

In this Letter, we present an ultrastable fiber-based time-domain CSP BHD, which can be applied in continuous variable quantum communication. The detector exhibits a gain of $3.2 \mu\text{V}$ per photon, common mode rejection ratio of above 76 dB, and signal-to-noise ratio above 20 dB. Optical pulses with repetition rates up to 2 MHz can be measured with a detection

*Supported by the National Natural Science Foundation of China (NSFC) (11074156), the TYAL, the National Key Basic Research Program of China (2010CB923101), the NSFC Project for Excellent Research Team (61121064), and the Shanxi Scholarship Council of China.

**Corresponding author. Email: yongmin@sxu.edu.cn

© 2012 Chinese Physical Society and IOP Publishing Ltd

efficiency of 66%. The stability of the detector in various time scales is studied by using Allan variance, and the superior stability of the detector enables a 100-s window for measurement without calibration.

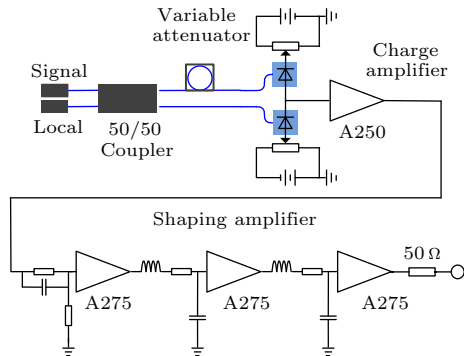


Fig. 1. The schematic diagram of the fiber-based time-domain BHD.

The schematic diagram of the CSP BHD is shown in Fig. 1. The signal and local oscillator (LO) pulses interfere at a 50/50 fiber splitter. For a shot-noise-limited BHD, high CMRR is critical and this means that the optical power of the two output pulses of the fiber splitter should be precisely balanced. In our experiment, a high balanced 50/50 fiber splitter with two equal-length output fiber pigtailed was adopted. To compensate for the slight imbalance of the beam splitter and that of the photodiodes quantum efficiency, a variable optical attenuator (VOA) based on bending the fiber was utilized,^[11,17] where the variable attenuation was achieved by changing the radius of the bending fiber. Furthermore, to balance the slightly different arrival times of the incident optical pulses, the photodiodes response can be precisely tuned by adjusting their bias voltage. Due to the junction capacitance of the photodiode, there exists a delay between the incident optical signal and the converted electric signal. By varying the applied bias voltage, the junction capacitance can be easily tuned and this will further modify the delay. The techniques adopted above do not need excess optical components which will introduce more losses and instability, and have the merits of high precision and superior stability.

In order to decrease the electronic noises from the power supply, we used batteries to provide the bias voltages to the InGaAs photodiodes (Thorlabs, FGA04). To minimize the parasitic capacitance the pins of the photodiodes should be cut as short as possible and close to the CSP. Due to the low dark current (below 1 nA), the common terminals of the photodiodes were connected directly to the input of the charge amplifier (Amptek A250) to achieve a lower electronic noise instead of connecting through a capacitance.^[9] When a capacitance is employed, the bias voltages of the photodiodes are not only determined by the battery voltage, but also affected by the capacitor. The

bias voltage will drift during the charging and discharging of the capacitor; such effect will induce instability of the detector. The difference current from the photodiodes was integrated by the CSP and an electrical pulse was generated. The electrical pulse was further transformed to a Gaussian shaped pulse by a shaping network (Amptek A275). To achieve a good output pulse shape, the photodiodes were carefully selected with almost identical response functions which are also important for a high CMRR. The output terminal terminated with a 50 Ω resistor. To avoid electromagnetic interference from the environment, the detector was enclosed in a shielding metal box.

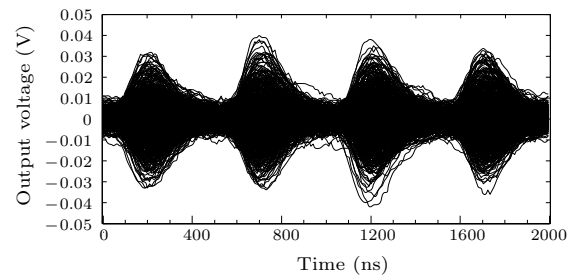


Fig. 2. Time traces of the homodyne detector output at a repetition rate of 2 MHz (The LO power is 5.7×10^6 photons per pulse).

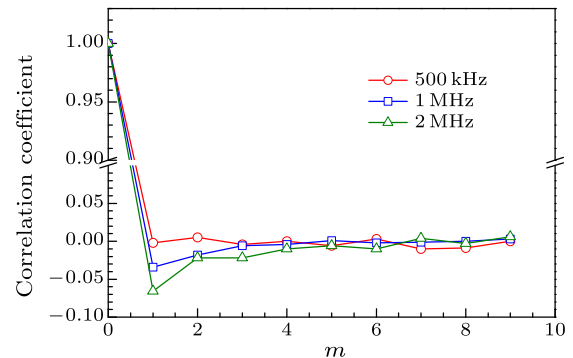


Fig. 3. Correlation coefficient at different repetition rates for vacuum field input.

To evaluate the BHD's performance, a 1550 nm single frequency pulsed laser was employed. Figure 2 shows typical time-traces of the detector for vacuum state input. The input optical field has a pulse width of 100 ns and a repetition rate of 2 MHz. The full width of the output electrical pulse is about 500 ns. From Fig. 2 we can see that the mean value of the output electric pulse is zero. If the output pulses of the fiber splitter are not balanced, the mean value will depart from zero. This zero-point drift can be solved using the VOA. If the arrival times of the incident optical pulses are not consistent, the upper part and lower part of the traces in Fig. 2 will separate along the time axis and it can be recovered by adjusting the bias voltage. The peak value of each electrical pulse gives a quadrature measurement for the signal field

with a gain of $3.2 \mu\text{V}$ per photon. The total detection efficiency and CMRR of the detector are measured to be 66% and 76 dB, respectively.

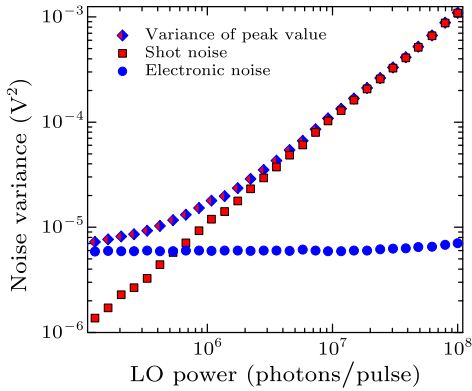


Fig. 4. The output peak value variance of the detector versus the LO power for vacuum field input.

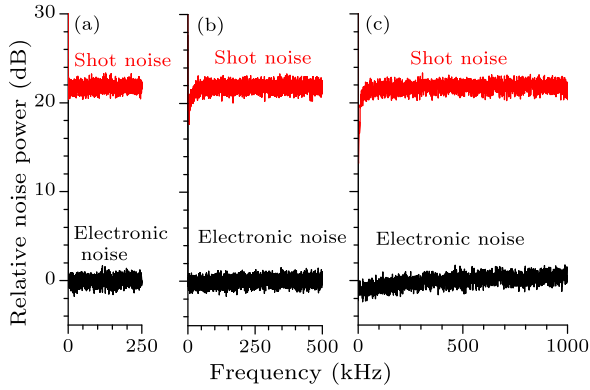


Fig. 5. The frequency spectra of the detector at different repetition rates with an LO power of 5×10^7 photons per pulse: (a) 500 kHz, (b) 1 MHz, (c) 2 MHz.

To check the time resolving power of the detector, the correlation coefficient (CC) between adjacent pulses was calculated.^[12] The quadratures of 5009 vacuum field pulses were recorded with the measured values $N(j)$ ($j = 1, 2, \dots, 5009$), and the CC is defined as

$$\text{CC}(m) = \frac{E(X(k)Y(k)) - E(X(k))E(Y(k))}{\sqrt{E(X(k)^2) - E^2(X(k))}\sqrt{E(Y(k)^2) - E^2(Y(k))}}, \quad (1)$$

where $X(k) = N(k)$ and $Y(k) = N(k + m)$ ($k = 1, 2, \dots, 5000$; $m = 0, 1, \dots, 9$). Figure 3 depicts the CC at different repetition rates (the shot noise to electronic noise ratio is 10 dB). It can be seen that there is a negative CC when the repetition rate is higher than 500 kHz, e.g., the CC between consecutive pulses ($m = 1$) is -0.065 at repetition rate of 2 MHz. For the repetition rate of 500 kHz, the CC decreases down to the order of ± 0.01 . In this situation, it is observed that the small correlation between two adjacent pulses is random and it is attributed to the statistical fluctu-

ations due to the limited number of samples and the electronic noise correlation of the detector.

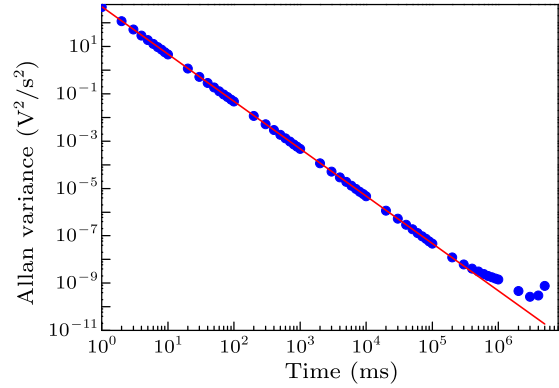


Fig. 6. Allan variance of the peak value of the detector output pulse.

The output peak value variance as a function of the LO power for vacuum signal input is shown in Fig. 4, where each data point was calculated from 50000 pulses. It is clear that the peak value variance scales with the LO power after subtraction of the electrical noise background. For a wide range of LO power spanning more than 2 orders of magnitude, the detector can work well in the linear region up to 10^8 photons per pulse and the shot noise to electronic noise ratio can reach above 20 dB. Figure 5 shows the noise spectra of the BHD at laser repetition rates of 500 kHz, 1 MHz, and 2 MHz. For a laser repetition rate of 500 kHz, the observed noise spectrum is flat in the frequency range from DC to half the repetition rate which indicates the noise observed is frequency independent (white). The dips in the low frequency part of the spectrum for the 1 MHz and 2 MHz repetition rates are due to the correlations of the adjacent electrical pulses. The test results given above confirm that our BHD is shot noise limited.

The BHD's long term stability is essential to determine how long the detector can work accurately without calibrating the low-frequency drift of the detector balance. The stability of the detector in various time scales is analyzed by using Allan variance defined by

$$\sigma^2(n\tau_0, N) = \frac{1}{2n^2\tau_0^2(N-2n)} \sum_{i=0}^{N-2n-1} (x_{i+2n} - 2x_{i+n} + x_i)^2, \quad (2)$$

where x_i is the measured quadrature value, τ_0 is the time interval between the adjacent sampling points, and N is the total number of samples. This technique is called the overlapped estimator, it has been accepted as the preferred Allan variance estimator.^[18] We acquired the data at a rate of 1 kHz for about three hours. Then different n is used to calculate the Allan variance in different time scales, as shown in Fig. 6.

The solid line is a linear fit using the data points for time less than 10 s, and we can see that the BHD has a 100 s window for accurate measurement without calibration. The departure due to the low-frequency drift of the detector balance begins at the time of around 200 s which is several orders higher than the results reported before.^[15,16]

In summary, we have demonstrated a fiber-based time-domain shot noise limited balanced homodyne detector. The detector exhibits a common mode rejection ratio above 76 dB, signal-to-noise ratio above 20 dB. Optical pulses with repetition rates up to 2 MHz, which is to date the highest repetition rate for the CSP BHD, can be measured with shot noise limited sensitivity. The superior stability of the detector enables a 100-s window for measurement without calibration. The detector presented will find useful applications in precision measurement of pulsed quantum light fields and in all-fiber continuous variable quantum information processing including quantum communication, etc.

References

- [1] Grosshans F et al 2003 *Nature* **421** 238
- [2] Lodewyck J et al 2007 *Phys. Rev. A* **76** 042305
- [3] Qi B et al 2007 *Phys. Rev. A* **76** 052323
- [4] Fossier S et al 2009 *New J. Phys.* **11** 045023
- [5] Smithey D T et al 1993 *Phys. Rev. Lett.* **70** 1244
- [6] Breitenbach G, Schiller S and Mlynek J 1997 *Nature* **387** 471
- [7] Zavatta A, Viciani S and Bellini M 2006 *Laser Phys. Lett.* **3** 3
- [8] Lvovsky A I and Raymer M G 2009 *Rev. Mod. Phys.* **81** 299
- [9] Hansen H et al 2001 *Opt. Lett.* **26** 1714
- [10] Wenger J, Brouri R T and Grangier P 2004 *Opt. Lett.* **29** 1267
- [11] Legre M, Zbinden H and Gisin N 2006 *Quantum Inf. Comput.* **6** 326
- [12] Chi Y M et al 2011 *New J. Phys.* **13** 013003
- [13] Zavatta A et al 2002 *J. Opt. Soc. Am. B* **19** 1189
- [14] Okubo R et al 2008 *Opt. Lett.* **33** 1458
- [15] Haderka O et al 2009 *Appl. Opt.* **48** 2884
- [16] Cooper M, Soller C and Smith B J 2011 arXiv: 1112.0875v1[quant-ph]
- [17] Lodewyck J et al 2005 *Phys. Rev. A* **72** 050303(R)
- [18] Snyder J J 1981 *Proc. 35th Annual Symposium on Frequency Control* (Philadelphia, Pennsylvania 27–29 May 1981) p 464

Chinese Physics Letters

Volume 29

Number 12

December 2012

GENERAL

- 120201 **Application of the Binary Bell Polynomials Method to the Dissipative (2+1)-Dimensional AKNS Equation**
LIU Na, LIU Xi-Qiang
- 120202 **Wave Interaction and Resonance in a Non-Ideal Gas**
Rajan Arora, Mohd. Junaaid Siddiqui, V. P. Singh
- 120301 **Quantum Fidelity and Thermal Phase Transitions in a Two-Dimensional Spin System**
WANG Bo, HUANG Hai-Lin, SUN Zhao-Yu, KOU Su-Peng
- 120302 **Violation of Leggett–Garg Inequalities in Single Quantum Dots**
SUN Yong-Nan, ZOU Yang, GE Rong-Chun, TANG Jian-Shun, LI Chuan-Feng
- 120303 **Quantum Stackelberg Dupoly with Continuous Distributed Incomplete Information**
WANG Xia, HU Cheng-Zheng
- 120501 **Propagation of Spiking and Burst-Spiking Synchronous States in a Feed-Forward Neuronal Network**
ZHANG Xi, HUANG Hong-Bin, LI Pei-Jun, WU Fang-Ping, WU Wang-Jie, JIANG Min
- 120502 **Generalized Zero-Temperature Glauber Dynamics in a Two-Dimensional Square Lattice**
MENG Qing-Kuan, FENG Dong-Tai, GAO Xu-Tuan, MEI Yu-Xue
- 120503 **Nonlocal Symmetry of the Lax Equation Related to Riccati-Type Pseudopotential**
WANG Yun-Hu, CHEN Yong, XIN Xiang-Peng
- 120504 **Quantum Friction**
Roumen Tsekov
- 120505 **Anti-Synchronization of Chaotic Systems via Adaptive Sliding Mode Control**
Wafaa Jawaada, M. S. M. Noorani, M. Mossa Al-sawalha
- 120701 **Acoustic Nonlinearity of a Laser-Generated Surface Wave in a Plastically Deformed Aluminum Alloy**
KIM Chung-Seok, JHANG Kyung-Young
- 120702 **High Performance Micro CO Sensors Based on ZnO-SnO₂ Composite Nanofibers with Anti-Humidity Characteristics**
YUE Xue-Jun, HONG Tian-Sheng, XIANG Wei, CAI Kun, XU Xing

THE PHYSICS OF ELEMENTARY PARTICLES AND FIELDS

- 121101 **An Anomaly Associated with Ward–Takahashi Identity for Pseudo-Tensor Current in QED**
BAO Ai-Dong, SUN Yi-Qian, WANG Dan

NUCLEAR PHYSICS

- 122101 **Photon Linear Polarization Coefficient of the Radiative Capture Process ${}^2\text{H}(p, \gamma){}^3\text{He}$ at Thermal Energies**
H. Sadeghi
- 122102 **Effect of Short-Range and Tensor Force Correlations on High-Density Behavior of Symmetry Energy**
XU Chang, REN Zhong-Zhou
- 122301 **The Neutrino Energy Loss by Electron Capture of Nuclides ${}^{52,53,54,55,56}\text{Fe}$ in Core-Collapse Supernova**
LIU Jing-Jing

ATOMIC AND MOLECULAR PHYSICS

- 123101 **Stereodynamics Study of $\text{Li}+\text{HF}/\text{DF}/\text{TF}\rightarrow\text{LiF}+\text{H}/\text{D}/\text{T}$ Reactions on X^2A' Potential Energy Surface**
TAN Rui-Shan, LIU Xin-Guo, HU Mei

- 123201 **Experimental Determination (\sim mHz) of the Ground-State Hyperfine Separation of Trapped $^{199}\text{Hg}^+$ in a Hyperbolic Paul Trap**
HE Yue-Hong, SHE Lei, CHEN Yi-He, YANG Yu-Na, LIU Hao, LI Jiao-Mei

FUNDAMENTAL AREAS OF PHENOMENOLOGY(INCLUDING APPLICATIONS)

- 124201 **The 1×4 Optical Splitters Based on Silicon Photonic Crystal Self-Collimation Ring Resonators**
ZHUANG Dong-Xia, CHEN Xi-Yao, LI Jun-Jun, QIANG Ze-Xuan, JIANG Jun-Zhen, CHEN Zhi-Yong, QIU Yi-Shen, LI Hui
- 124202 **Ultrastable Fiber-Based Time-Domain Balanced Homodyne Detector for Quantum Communication**
WANG Xu-Yang, BAI Zeng-Liang, DU Peng-Yan, LI Yong-Min, PENG Kun-Chi
- 124203 **Information Transferring between a Photon's Orbital Angular Momentum and Frequency**
LIU Rui-Feng, ZHANG Pei, GAO Hong, LI Fu-Li
- 124204 **A Switchable Multi-wavelength Erbium-Doped Photonic Crystal Fiber Laser with Linear Cavity Configuration**
ZHENG Wan-Jun, CHENG Jian-Qun, RUAN Shuang-Chen, ZHANG Min, LIU Wen-Li, YANG Xi, ZHANG Ying-Ying
- 124205 **Terahertz Wave Confinement in Pillar Photonic Crystal with a Tapered Waveguide and a Point Defect**
WANG Chang-Hui, KUANG Deng-Feng, CHANG Sheng-Jiang, LIN Lie
- 124206 **A Switchable and Tunable Dual-Wavelength Actively Mode-Locked Fiber Laser Based on Dispersion Tuning**
MEI Jia-Wei, XIAO Xiao-Sheng, GUI Li-Li, XU Ming-Rui, YANG Chang-Xi
- 124207 **Three-Dimensional Hermite-Bessel-Gaussian Soliton Clusters in Strongly Nonlocal Media**
JIN Hai-Qin, LIANG Jian-Chu, CAI Ze-Bin, LIU Fei, YI Lin
- 124208 **Analytic Solutions for the Spectral Responses of RCA-Grating-Based Waveguide Devices**
ZENG Xiang-Kai, WEI Lai
- 124209 **The Generation Mechanism of Airy-Bessel Wave Packets in Free Space**
REN Zhi-Jun, YING Chao-Fu, FAN Chang-Jiang, WU Qiong
- 124210 **Blue-Extended Supercontinuum Generation in Photonic Crystal Fibers with Picosecond Pulse Pumping**
ZHU Xian, ZHANG Xin-Ben, CHEN Xiang, PENG Jing-Gang, DAI Neng-Li, LI Jin-Yan
- 124211 **Temporal, Spectral and Spatial Characterization of High-Energy Laser Pulse with Small Bandwidth Propagating through Long Path**
DENG Xue-Wei, WANG Fang, JIA Huai-Ting, XIANG Yong, FENG Bin, LI Ke-Yu, ZHOU Li-Dan
- 124212 **Adaptive Polarization Control of Fiber Amplifier Based on SPGD Algorithm**
XIONG Yu-Peng, SU Rong-Tao, LI Xiao, HOU Pu, WANG Xiao-Lin, XU Xiao-Jun
- 124301 **Analysis of Imperfect Acoustic Cloaking Resonances**
KIM Seungil
- 124302 **Monte Carlo Simulation of Scattered Light with Shear Waves Generated by Acoustic Radiation Force for Acousto-Optic Imaging**
LU Ming-Zhu, WU Yu-Peng, SHI Yu, GUAN Yu-Bo, GUO Xiao-Li, WAN Ming-Xi
- 124701 **Mixed Convection Heat Transfer in Micropolar Nanofluid over a Vertical Slender Cylinder**
Abdul Rehman, S. Nadeem
- 124702 **The Normalized Analysis of a Surface Heterogeneous Reaction of a Propane/Air Mixture into a Micro-Channel**
A. Fanaee, J. A. Esfahani

PHYSICS OF GASES, PLASMAS, AND ELECTRIC DISCHARGES

- 125201 **Temperature Characteristics of Cathode Sheath in High-Pressure Volume Discharge Derived from Emanating Shock Wave**
YANG Chen-Guang, XU Yong-Yue, ZUO Du-Luo

CONDENSED MATTER: STRUCTURE, MECHANICAL AND THERMAL PROPERTIES

- 126101 Determination of the Lattice Parameters of a Si Nanobelt in a Tensile Test Process Using an MEMS Actuator**
ZENG Hong-Jiang, LI Tie, JIN Qin-Hua, XU Fang-Fang, WANG Yue-Lin
- 126102 Growth of Self-Catalyzed InP Nanowires by Metalorganic Chemical Vapour Deposition**
LV Xiao-Long, ZHANG Xia, YAN Xin, LIU Xiao-Long, CUI Jian-Gong, LI Jun-Shuai, HUANG Yong-Qing, REN Xiao-Min
- 126103 A Raman Study of the Origin of Oxygen Defects in Hexagonal Manganite Thin Films**
CHEN Xiang-Bai, HIEN Nguyen Thi Minh, YANG In-Sang, LEE Daesu, NOH Tae-Won
- 126801 A Potential Hydrogen-Storage Media: C₂H₄ and C₅H₅ Molecules Doped with Rare Earth Atoms**
LEI Hong-Wen, ZHANG Hong, GONG Min, WU Wei-Dong
- 126802 Modification of Optical Band Gap and Surface Morphology of NiTsPc Thin Films**
Muhamad Saipul Fakir, Zubair Ahmad Khaulah Sulaiman

CONDENSED MATTER: ELECTRONIC STRUCTURE, ELECTRICAL, MAGNETIC, AND OPTICAL PROPERTIES

- 127101 New Method to Deal with Three-Dimensional Electron Gas with a Strong Correlation Effect**
YU Zhi-Ming, GUO Qian, LIU Yu-Liang
- 127102 Influence of Oxygen Partial Pressure on the Fermi Level of ZnO Films Investigated by Kelvin Probe Force Microscopy**
SU Ting, ZHANG Hai-Feng
- 127103 Influence of Pressure on the Structural, Electronic and Mechanical Properties of Cubic SrHfO₃: A First-Principles Study**
FENG Li-Ping, WANG Zhi-Qiang, LIU Qi-Jun, TAN Ting-Ting, LIU Zheng-Tang
- 127104 A New Method to Calculate the Rashba Spin Splitting in III-Nitride Heterostructures**
LI Ming, SUN Gang, FAN Li-Bo
- 127201 Onset for the Electron Velocity Overshoot in Indium Nitride**
Clóves G. Rodrigues
- 127301 Analysis of Off-State Leakage Current Characteristics and Mechanisms of Nanoscale MOSFETs with a High-*k* Gate Dielectric**
LIU Hong-Xia, MA Fei
- 127302 Laser-Induced Indium-Diffusion into Cadmium Sulfide Thin Film for Solar Cell Applications**
KIM Nam-Hoon, MYUNG Kuk Do, LEE Woo-Sun
- 127303 GaSb p-Channel Metal-Oxide-Semiconductor Field-Effect Transistors with Ni/Pt/Au Source/Drain Ohmic Contacts**
WU Li-Shu, SUN Bing, CHANG Hu-Dong, ZHAO Wei, XUE Bai-Qing, ZHANG Xiong, LIU Hong-Gang
- 127304 Ultracompact Refractive Index Sensor Based on Surface-Plasmon-Polariton Interference**
WANG Chen, CHEN Jian-Jun, TANG Wei-Hua, XIAO Jing-Hua
- 127305 Enhanced Photovoltaic Properties of Gradient Doping Solar Cells**
ZHANG Chun-Lei, DU Hui-Jing, ZHU Jian-Zhuo, XU Tian-Fu, FANG Xiao-Yong
- 127501 Influence of Film Roughness on the Soft Magnetic Properties of Fe/Ni Multilayers**
LUO Zhi-Yuan, TANG Jia, MA Bin, ZHANG Zong-Zhi, JIN Qing-Yuan, WANG Jian-Ping
- 127601 Preparing Pseudo-Pure States in a Quadrupolar Spin System Using Optimal Control**
TAN Yi-Peng, NIE Xin-Fang, LI Jun, CHEN Hong-Wei, ZHOU Xian-Yi, PENG Xin-Hua, DU Jiang-Feng
- 127701 Ultrasonic Energy Transference Based on an MEMS ZnO Film Array**
WU Shao-Hua, ZHAO Zhan, ZHAO Jun-Juan, GUO Li-Jun, DU Li-Dong, FANG Zhen, KONG De-Yi, XIAO Li, GAO Zhong-Hua
- 127801 A Novel Efficient Red Emitting Iridium Complex for Polymer Light Emitting Diodes**
HU Zheng-Yong, YANG Jian-Kui, LUO Jing, LIANG Min, WANG Jing

- 127802 An Improvement on the Junction Temperature Measurement of Light-Emitting Diodes by using the Peak Shift Method Compared with the Forward Voltage Method**
HE Su-Ming, LUO Xiang-Dong, ZHANG Bo, FU Lei, CHENG Li-Wen, WANG Jin-Bin, LU Wei
- 127803 The Evolution of Defects in Deformed Cu-Ni-Si Alloys during Isochronal Annealing Studied by Positron Annihilation**
QI Ning, JIA Yan-Lin, LIU Hui-Qun, YI Dan-Qing, CHEN Zhi-Quan
- 127804 Origin of Ferromagnetism in $Zn_{1-x}Co_xO$ Thin Films: Evidences Provided by Hard and Soft X-Ray Absorption Spectroscopy**
XI Shi-Bo, CUI Ming-Qi, QIN Xiu-Fang, XU Xiao-Hong, XU Wei, ZHENG Lei, ZHOU Jing, LIU Li-Juan, YANG Dong-Liang, GUO Zhi-Ying

CROSS-DISCIPLINARY PHYSICS AND RELATED AREAS OF SCIENCE AND TECHNOLOGY

- 128101 The High Nitrogen Pressure Synthesis of Manganese Nitride**
SI Ping-Zhan, JIANG Wei, WANG Hai-Xia, ZHONG Min, GE Hong-Liang, CHOI Chul-Jin, LEE Jung-Goo
- 128102 The Synthesis and Characterization of Peach-Like ZnO**
A. Kamalianfar, S. A. Halim, Siamak Pilban Jahromi, M. Navasery, Fasih Ud Din, K. P. Lim, S. K. Chen, J. A. M. Zahedi
- 128103 The Effects of Heating Mechanism on Granular Gases with a Gaussian Size Distribution**
LI Rui, XIAO Ming, LI Zhi-Hao, ZHANG Duan-Ming
- 128401 Independently Tunable Multichannel Filters Based on Graphene Superlattices with Fractal Potential Patterns**
ZHANG Hui-Yun, ZHANG Yu-Ping, GAO Ying, YIN Yi-Heng
- 128501 The Structural and Electrical Properties of Al/Pb($Zr_{0.52}Ti_{0.48}$) O_3 /Al $_2$ O $_3$ /Si with an Al $_2$ O $_3$ Layer Prepared by using the Molecular Atomic Deposition Method**
YANG Yi, ZHOU Chang-Jian, PENG Ping-Gang, XIE Dan, REN Tian-Ling, PAN Xiao, LIU Jing-Song
- 128502 A 50–60 V Class Ultralow Specific on-Resistance Trench Power MOSFET**
HU Sheng-Dong, ZHANG Ling, CHEN Wen-Suo, LUO Jun, TAN Kai-Zhou, GAN Ping, ZHU Zhi, WU Xing-He
- 128901 Topological and Spectral Perturbations in Complex Networks**
YAN Xin, WU Yang
- 128902 Pheromone Static Routing Strategy for Complex Networks**
HU Mao-Bin, Henry Y.K. Lau, LING Xiang, JIANG Rui
- 128903 Self-Similarity in Game-Locked Aggregation**
WANG Chao, XIONG Wan-Ting, WANG You-Gui

JUST FOR AUTHORS
— CHINESE PHYSICS LETTERS